

Full Length Research Paper

An experimental study on the flexural behavior of FRP RC beams and a comparison of the ultimate moment capacity with ACI

Iman Chitsazan¹, Mohsen Kobraei^{2*}, Mohd Zamin Jumaat² and Payam Shafigh²

¹Department of Civil Engineering, Babol Noshirvani University of Technology, Babol, Iran.

²Department of Civil Engineering, Faculty of Engineering, University of Malaya, 50603 Kuala Lumpur, Malaysia.

Accepted 4 November, 2010

As it is known, fiber reinforced polymer (FRP) bars are typically quite different from those of steel bars and they depend mainly on both matrix and fibers type, as well as on their volume fraction; although generally, FRP bars have lower weight, lower modulus of elasticity, but higher strength than steel. In the other hand, FRP has disadvantages, for instance: no yielding before brittle rupture and low transverse strength. In this research, we have investigated flexural behavior in reinforced concrete beams with glass fiber-reinforced polymer (GFRP) and have analyzed the different kinds of failure, ultimate moment capacity, deflection, load of first crack, how to create and expand cracks, tensile and compressive strains created on beam and position of neutral axis (NA) during loading for different ratios of bars on 10 laboratorial specimens. Using high strength concrete instead of normal concrete and increasing the effective depth over the breadth on flexural behavior of concrete beams with GFRP had been studied. Results taken from the experimental tests have been compared with ACI 440 and they show that deflections, width of cracks and the cracks' extent are further used toward the usual RC beams. High strength concrete instead of normal concrete is the ascended load of the first crack and it created more cracks, but with less width of crack. It is recommended that the selected ratio of effective depth over breadth (d/b) is slightly larger than 2. In addition, it can be said that the amount of the balanced bar provided by ACI 400 is not an exact criteria to determine the type of failure, and it is only in cases where the ratio of bars are lower than the balanced mode that ruptures occur in reinforcement area.

Key words: Concrete beam, fiber reinforced polymer (FRP), flexural behavior, ultimate moment, deflection.

INTRODUCTION

For years, civil engineers have been searching alternatives to steels and alloys to combat the high costs of repair and maintenance of structures damaged by corrosion and heavy use. With progress made by the polymer industry in the world, researchers think that these materials should be used in building structures. Following their researches, the thought of using polymer materials instead of steel in concrete structures, led to the entry of fiber reinforced polymer (FRP) into field structures and constructions.

Fiber reinforced polymers (FRP) bars are non-corrosive

and as such, they have higher strength than their steel counterparts. Also, they have been used in aggressive environments such as water treatments plants instead of steel (AlMusallam et al., 1997; Alsayed, 1998, 1997; Benmokrane et al., 1995, 1996; Brown and Bartholomew, 1993; Deitz et al., 1999; Duranovic et al., 1997; Grace et al., 1998; Masmoudi et al., 1998; Michaluk et al., 1998; Pecce et al., 2000; Thériault and Benmokrane, 1998). The other merits of fiber reinforced polymer are derived from its light weight and non-magnetic characteristics (Thériault and Benmokrane, 1998; Yost et al., 2001; Tureyen and Frosch, 2002), but the use of these materials have been limited because of the low modulus of elasticity and low ductility of large creeps which these problems result to (Thériault and Benmokrane, 1998; Yost et al., 2001; Tureyen and Frosch, 2002;

*Corresponding author. E-mail: mkobraei@yahoo.com. Tel: +60-12-6687348.

Yost et al., 2001). Also, the lacks of ductility of the parts made, to include the lack of comprehensive codes and standards for these bars, are other disadvantages of these bars.

Researches done on concrete reinforced members with FRP show that, no yield stress was seen, bearing in mind the linear relation between stress and strain in FRP bars (Victor and Shuxin, 2002). Width and extent of cracks in these beams are further used in the steel specimens (Benmokrane et al., 1996; Vijay and GangaRao, 2001). Deflection of concrete beams with FRP also is very bigger than similar samples of RC beams with steel, around 4 times, and the diagram of their load-deflection is in a straight line (Saadatmanesh and Ehsani, 1991; Victor and Shuxin, 2002). In addition, the usage of high strength concrete is effective (Vijay and GangaRao, 2001; Yost and Gross, 2002). In some compressive rupture of these beams at ultimate loading, a descent of the neutral axis (N.A.) has been seen with an increase in loading (Vijay and GangaRao, 2001).

For the design of the flexural concrete reinforced members with FRP, various relations are presented with the basic assumptions of achieving these relations, and as such, they are used for the reinforced concrete members with steel bars (ACI Committee 440, 2001; Faza and GangaRao, 1993), and the properties of FRP are used as a replacement of the steel properties. In these relations, a ratio of the balanced mode is defined and the ratio that is higher and smaller than the balanced mode will cause the rupture in the compressive area. Of course, in cases where the ratio of bars is smaller than the balanced mode and the rupture in the compressive zone, it indicates that the submitted relation of the ratio of bars in the balanced mode is not the exact criteria for determining the kind of failure.

Importance of the study

In this study, flexural behavior of rectangular concrete beams reinforced with glass fiber-reinforced polymer (GFRP) will be examined with manufacturing 10 specimens. Considering the constant length and diameter of GFRP bars, various ratios of bars are investigated. The effect of the use of high strength concrete instead of normal concrete had been researched and they are compared with the reference samples without compression reinforcement. In addition, the effect of the increased effective depth over the breadth (d/b) for constant ratio of bars was investigated.

In this study, the type of failure, ultimate moment capacity of beams, creeps of beams, load of first crack, how to create and expand cracks, tensile and compressive strain and the position of the neutral axis for evaluating the flexural behavior of beams was compared and examined. To determine the exact criteria of the different kinds of rupture, manufactured beams have ratios of smaller bar than the balanced mode. Also, the

results taken from the experimental tests were compared with ACI 440 relations.

Relation of ACI 440 for design concrete beams with GFRP as reinforcement (ACI Committee 440, 2001)

Failure mode

The flexural capacity of an FRP reinforced flexural member is dependent on whether the failure is governed by concrete crushing or FRP rupture. The failure mode can be determined by comparing the FRP reinforcement ratio to the balanced reinforcement ratio (that is, a ratio where concrete crushing and FRP rupture occur simultaneously). Because FRP does not yield, the balanced ratio of FRP reinforcement is computed using its design tensile strength. The FRP reinforcement ratio can be computed from Equation (1) and the balanced FRP reinforcement ratio can be computed from Equation (2)

$$\rho_f = \frac{A_f}{bd} \quad (1)$$

$$\rho_{fb} = 0.85\beta_1 \frac{f'_c}{f_{fu}} \frac{E_f \epsilon_{cu}}{E_f \epsilon_{cu} + f_{fu}} \quad (2)$$

If the reinforcement ratio is less than the balanced ratio ($\rho_f < \rho_{fb}$), FRP rupture failure mode governs. Otherwise, ($\rho_f > \rho_{fb}$) concrete crushing governs. The balanced ratio for FRP reinforcement ρ_{fb} is much lower than the balanced ratio for steel reinforcement ρ_b . In fact, the balanced ratio for FRP reinforcement can be even lower than the minimum reinforcement ratio for steel.

Nominal flexural strength

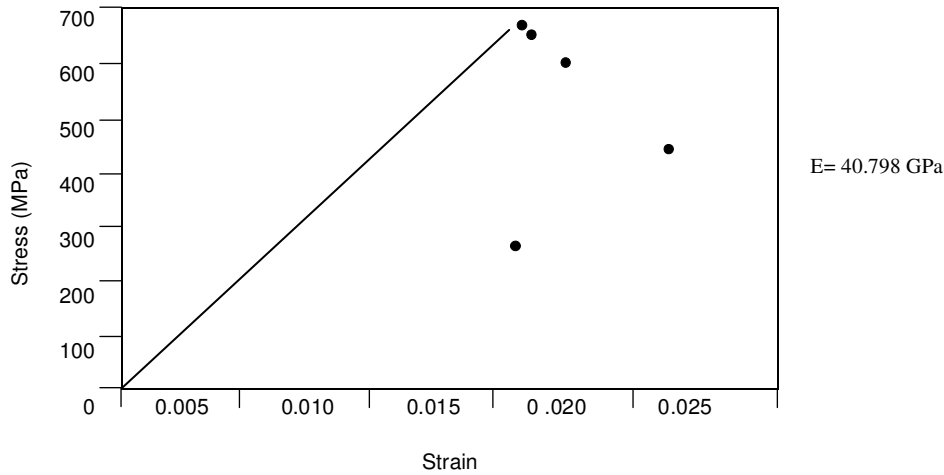
When $\rho_f > \rho_{fb}$, which is the failure of the member is initiated by crushing of the concrete, the stress distribution in the concrete can be approximated with the ACI rectangular stress block. Based on the equilibrium of forces and strain compatibility, the following can be derived:

$$M_u = \rho_f f_f (1 - 0.59 \frac{\rho_f f_f}{f'_c}) b d^2 \quad (3)$$

$$f_f = \left(\sqrt{\frac{(E_f \epsilon_{cu})^2}{4} + \frac{0.85\beta_1 f'_c}{\rho_f} E_f \epsilon_{cu}} - 0.5 E_f \epsilon_{cu} \right) \leq \rho_{fu} \quad (4)$$

Table 1. Properties of GFRP bar.

Number of bar	Diameter of bar	Area of bar	Modulus of elasticity	Ultimate tensile strain
	d_f (mm)	A_f (mm ²)	E_f (GPa)	f_{fu}^* (MPa)
# 4	12.7	126.7	40.81	690

**Figure 1.** Stress-strain.

When $\rho_f < \rho_{fb}$, the failure of the member is initiated by the rupture of the FRP bar, the ACI stress block is not applicable because the maximum concrete strain (0.003) may not be attained. In this case, an equivalent stress block is needed so that it approximates the stress distribution in the concrete at the particular strain level reached.

The analysis incorporates two unknowns: the concrete compressive strain at failure ϵ_c and the depth to the neutral axis c . In addition, the rectangular stress block factors, α_1 and β_1 , are unknown. The factor α_1 is the ratio of the average concrete stress to the concrete strength, while factor β_1 is the ratio of the depth of the equivalent rectangular stress block to the depth of the neutral axis. As such, the analysis involving all these unknowns becomes complex. Thus, the nominal flexural strength can be computed as shown in Equation (5)

$$M_n = 0.8A_f f_{fu} \left(d - \frac{\beta_1 c}{2} \right) \quad (5)$$

The product of $\beta_1 c$ in Equation (5) varies, depending on the material properties and FRP reinforcement ratio. The maximum value for this product is equal to $\beta_1 c_b$ and is achieved when the maximum concrete strain (0.003) is attained. A simplified and conservative calculation of the

nominal flexural strength of the member can be based on Equations (6) and (7) as follows:

$$M_n = 0.8A_f f_{fu} \left(d - \frac{\beta_1 c_b}{2} \right) \quad (6)$$

$$c_b = \left(\frac{\epsilon_{cu}}{\epsilon_{cu} + \epsilon_{fu}} \right) d \quad (7)$$

ACI, which is the coefficient of 0.8 in Equation (6), is considered to ensure the attainment of the strain.

MATERIALS AND METHODS

Materials properties

All FRP bars used in this study are of GFRP types, while specifications of GFRP are listed in Table 1. To create better adhesion between GFRP bars and concrete, two methods are used. The first one is wrapping glass fiber around reinforcement bars, and the second one is spraying sands over the surface of the reinforcement bars with silica glue. Figure 1 shows stress-strain graph of the reinforcement bars. However, the yield stress of steel bars is 300 MPa. To avoid shear failure, stirrups bars $\varnothing 6$ with 400 MPa have been used. Thus, steel bars of reference beams and $\varnothing 20$ with 300 MPa yield stress are rebarred. In reference beams, the

Table 2. Properties of compressive steel bars.

Diameter of bars	Area of bars	Modules of elasticity	Yield strain	Rupture strain
$d_s (mm)$	$A_s (mm^2)$	$E_s (GPa)$	$f_y (MPa)$	$f_u (MPa)$
6	28.3	200	400	600
20	314	200	300	500

Table 3. Properties of mix design for normal and high strength concrete (kg).

Kind of concrete	Cement	Water	Gravel	Sand	Super plasticizer	Micro silica	Weight ratio of water to cement
Normal	450	235	980	810	-	-	0.52
H. strength	450	150	980	810	10	50	0.33

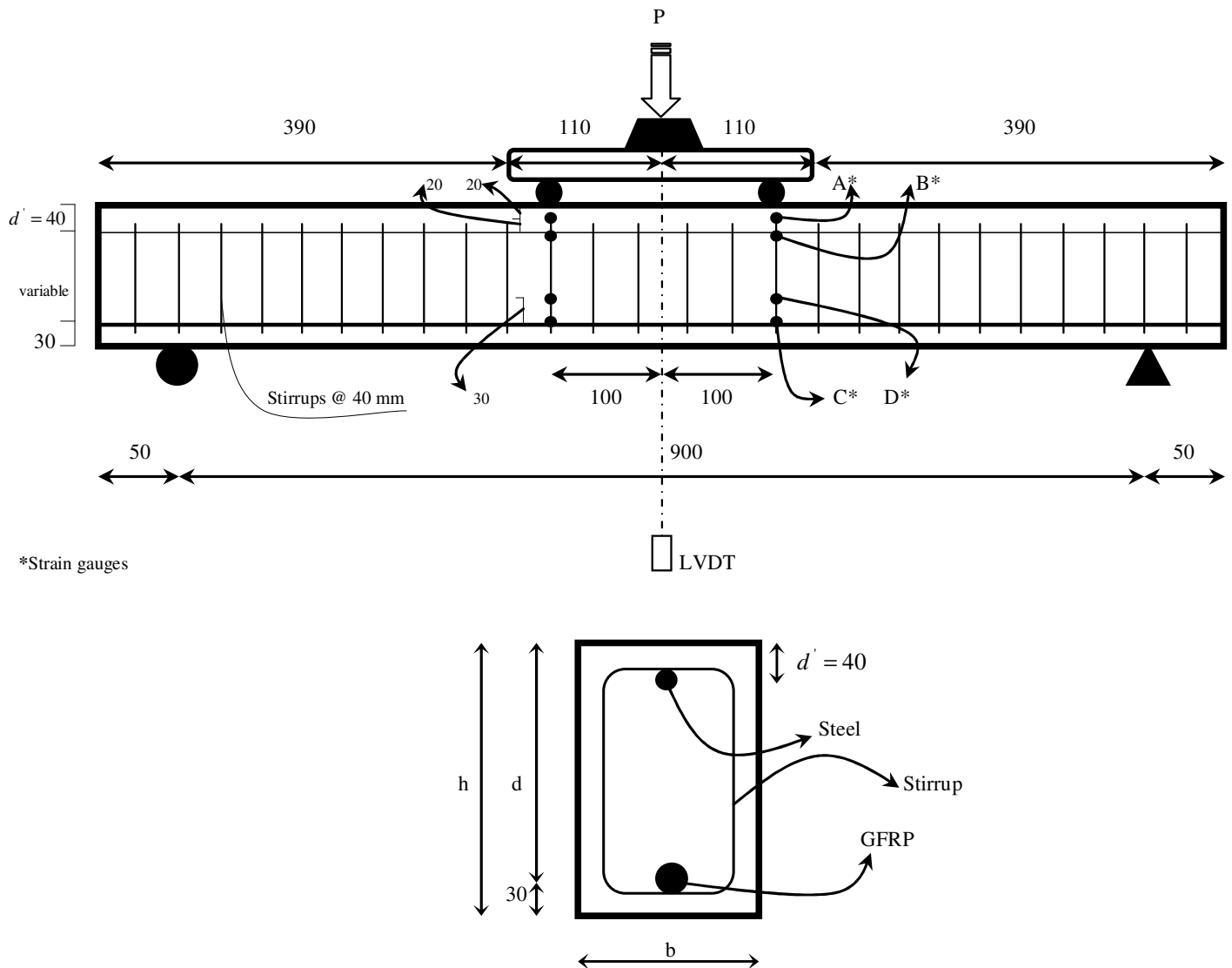


Figure 2. Schematic shape of the beam (mm).

multiplied diameter of the steel bars in yield stress is equal to the multiplied diameter of the FRP bars in the yield stress of FRPs. Moreover, the profile of steel bars used is given in Table 2.

In this research, two categories of concrete have been used. The first one is the nominal resistance with 40 MPa and the other one is the high strength concrete with 70 MPa. Type 2 of Portland cement is used and the diameter of the largest grain is 9.5 mm. Table 3 shows mix design of materials consumed to produce one cubic meter of concrete.

Specimens

In our study, 10 beams have been made and tested. While the length of all beams used to achieve various ratios of bars is 90 cm, the variable sizes are considered due to the constant diameter of FRP bars. NCF is the name of the beams with tensile FRP bars and normal concrete, and as such, the beams called HCF are similar to the NCF with a difference. Instead, the normal concrete replaced high strength concrete. Beams which have characterized NCF are considered as reference samples and are made from steel bars instead of FRP as tensile reinforcements. In these beams, the multiplied yield stress in the area of bars had been selected closely to the multiplied yield stress of FRP in the area of FRPs.

Concrete reinforced beams with FRP are designed based on ACI 440 rules and regulations (ACI Committee 440, 2001) and most of them with the ratio of bars less than the balanced condition for rupture were designed from the reinforcement region. As such, only NCF4 had ratio of bars more than the balanced state. Also, NCS group had been designed based on ACI 318 (ACI Committee 318, 1999) with the ratio of bars less than the balanced condition.

For assembly, stirrups are used as a steel wire with 2 mm diameters. Details of specimens made were given in Figure 2 and Table 4. Beams made are gotten from molds after 24 h, and they have been kept in the laboratory under wet sacks and big plastic bags for 28 days. After this period, samples were stored in the laboratory and after 105 days, beams were tested. Also, during casting, the determination of the compressive strength of concrete beams from the concrete prepared, have been sampled.

Experimental program

Schematic view and a view of the test set-up are shown in Figure 2. The beams with 900 mm clear span were simply supported and subjected to two concentrated static loads with 110 mm distance from each other. A concrete clear cover of 30 mm was kept constant for all the test-beams. Steel stirrups of 6 and 8 mm diameter were used at 400 mm spacing along the tested length for all beams. A device for measuring deflection is placed in the middle of beams.

RESULTS AND DISCUSSION

Investigation of beams failure

The beam is called NCF1 with FRP tensile reinforcement and ratio $\rho_f = 0.00487 = 0.555\rho_{fb}$. At 23.466 kN, the first flexural crack appeared between two loads. With the increasing load, other flexural cracks were created also between the two loads. The shear cracks with a very large slope outside the distance of two loads and close to the applied point loads were created. At load 180 kN, a large shear crack with almost 45° from supports were

created. Finally, the beam at load 197.71 kN was destroyed in the middle of the beam due to failure in the compressive region.

The NCF2 with a ratio of FRP bars $\rho_f = 0.00745 = 0.849\rho_{fb}$ is a little bigger than NCF1.

However, this increase had been achieved with constant diameters of reinforcements and reduction in size. The first crack appeared in the mid-span at 15.349 kN loading. When more loads were applied, the shear cracks with a large slope outside the two loads that is distant and closer to them were created. Then, at about 130 kN, the compressive concrete was breaking. Finally, at 141.11 kN, the compressive zone was totally broken and the beam was divided into two parts and the reinforcement was damaged as well.

The ratio of NCF3 was similar to NCF2, but the ratio of effective depth over breadth was larger. This ratio was selected as 2/11 when the first crack on this beam at 12.5 kN bending region happened. It should be noted that there were no cracks from 20 to 38 kN. Finally, the compressive region began to obliterate at 134.95 kN.

In NCF4, different dimensions have been decreased and the ratio of FRP reinforcement is higher than the level of the balanced mode. This ratio is equal to $\rho_f = 0.00990 = 1.13\rho_{fb}$. The first crack on this beam,

at 9.642 kN, in the bending region happened close to the bending area. With increasing loading at 100.94 kN, the concrete of the compressive zone got broken.

Beam HCF5 is similar to NCF1 with a difference that the compressive steel bar was used to manufacture the beam. The load of the first crack happened in the mid-span at 42 kN. As such, the cracking patterns are same as NCF1. After increasing loading, cracks width was bigger, and at 150.1 kN, the beam suddenly got broken and we had failure in concrete reinforcement.

Beam HCF6 is similar to NCF2 with a difference in concrete strength. The load of the first crack happened at 16.667 kN in the bending area and was closer to one of the loads. With the growing loading cracks, widths were smaller and further expanded in comparison with NCF2, but their shape was the same. At 127.48 kN, compressive concrete was destroyed, and under the destroyed region, a crack with large width was created.

Beam HCF7 is similar to NCF3 in the strength of concrete and the first crack appeared in the mid-span at 18.203 kN. The number and extension of cracks had been seen more than the one in NCF3. After increasing loading at 154.05 kN, in an applied load position, the crack was broken into two parts and these show that we had failure in the compressive region to include reinforcement at the same time.

Beam HCF8 is similar to NCF4 and the only difference is the strength of the concrete which is bigger than NCF4. As such, the first crack was seen at 13.81 kN and the number and extension of cracks were more than the NCF4 one. With increase in the loading at 106.42 kN, the concrete of the compressive area started to fail. After

Table 4. Properties of specimens.

Beams	Effective length	Breadth	Depth	Effective depth	Size of tensile steel bars	Ratio of bar	Ratio of bar Tensile balanced mode	Distance of steel bars (mm)	Strength of concrete
	$l_e (m m)$	$b(mm)$	$d(mm)$	$d_e(mm)$		ρ	ρ_b		f_c'
NCF1	900	130	230	200	# 4	0.00487	0.00878	6@40	41.4
NCF2	900	100	200	170	# 4	0.00745	0.00878	6@40	41.4
NCF3	900	90	220	190	# 4	0.00741	0.00878	6@40	41.4
NCF4	900	80	190	160	# 4	0.00990	0.00878	6@40	41.4
HCF5	900	130	230	200	# 4	0.00487	0.01343	6@40	73.9
HCF6	900	100	200	170	# 4	0.00745	0.01343	6@40	73.9
HCF 7	900	90	220	190	# 4	0.00741	0.01343	8@40	41.4
HCF 8	900	80	190	160	# 4	0.00990	0.01343	8@40	41.4
NCF15	900	130	230	200	# 20	0.01208	0.04190	8@40	41.4
NCF16	900	100	200	170	#20	0.01847	0.04190	8@40	41.4

removing the load, the beam showed totally, an elastic behavior and returned to its original state, while the compressive concrete fell off only. Beam HCF9 is similar to NCF1 with a difference, in that we used the compressive steel bar to manufacture this beam. The load of the first crack happened in the mid-span at 25.879 kN of which their difference can be denied, and as such, the cracking patterns are same as NCF1. After increasing loading cracks, the width was bigger and at 170.28 kN, the reinforcement bar was suddenly broken, but because of the compressive steel bar, it is unlikely that the compressive steel bar were not broken in two parts. We can see that in this beam, using compressive steel bar has changed the beam failure and concrete rupture. Beam HCF10 is similar to NCF2 with this difference, because we used the compressive steel bar to make this beam.

The load of the first crack happened at 13.8 kN in the bending area and close to one of the loads. With the growing loading cracks, the widths were smaller and further expanded in comparison to

NCF2, but their shapes were the same. At 110.37 kN, the compressive concrete was destroyed and under the destroyed region, a crack with large width was created. After removing the load, the beam did not come back to the original state and a significant amount of the creep due to loading has remained. The reason is that the compressive steel bars changed the elastic behavior of the reinforced concrete beam with FRP.

The NCF15 is similar to NCF1 with this difference, because we used steel bar instead of FRP as reinforcement. The first crack was flexural and it appeared at 40 kN more than NCF1 and close to HCF5. As such, the number and extension of cracks were less than FRP reinforced concrete beam. However, there was no crack from 40 to 70 kN. Finally, rupture occurred in the compressive concrete at 246.9 kN.

Beam HCF16 is similar to NCF2 and the only difference was the used steel bar instead of FRP as reinforcement. The first crack was seen at 25 kN and it was significantly bigger than the FRP concrete beams. As such, the number and

extension of cracks has been seen less than the FRP reinforced concrete beam. From 25 to 50 kN, no crack occurred. With increase in loading at 167.22 kN, the reinforcement was destroyed.

With assessment of cracks, it is seen that the load of the first crack will be decreased if the diameter of FRP can be constant. Also, the use of high strength concrete increases the load of the first crack significantly. In beams with similar ratios of bars and same strength of concrete, changing the size of sections do not have significant effect on cracks, but the usage of high strength concrete is replaced in the normal concrete. In the FRP reinforced concrete, the beams caused an increase in the numbers and extent of cracks, while it caused a reduction in the width of cracks. In addition, the rise of effective depth over breadth in the manufactured beam from normal concrete and constant ratios of FRP bars cause an increase in the numbers and extent of cracks, but in the beams made from high strength concrete, it did not have any significant effect on them. As an example, the types

rupture in eight beams are given in Figure 3.

Analysis of deflections

The diagram of load-deflection on mid-span is shown in Figure 4 and it can be observed that the deflection at mid-span in concrete beams with FRP is also very bigger than similar samples of RC beams with steel, around 4 times. Likewise, the diagram of load-deflection in the reinforced concrete beams with FRP almost looks like a straight line with light slope, unlike the diagram of load-deflection at mid-span in regular RC beams, which started with high slope; and after failure of the steel, the slope of the diagram became light unexpectedly. It is said that the diagram in RC beams with FRP almost looks like a straight line with light slope. This reason shows totally, the elastic behavior of FRP and gives the elastic behavior to the beams.

As it is noted in the figures, the general shape of load-deflection at mid-span with similar dimensions and ratios of bars are so close together and the usage of high strength concrete has not created major changes. In the load-deflection diagram of the normal concrete, the beams are closer to the straight line, but in the diagram of the high strength concrete, the beams are located with a very little twist around the diagram of the normal concrete and in some loads, it has more deflection while in some, it has less deflection.

In general, it can be said that the increase strength of concrete does not notably affect the deflection of reinforced concrete beams with FRP. Also, a reduction of the section's dimension in the constant ratio of bars is caused by a notable deflection in the reinforced beams with FRP and this case is clear in all modes. In addition, increase of the effective depth over breadth (d/b) in all cases has been reasoned as a decrease of beams deflection. Therefore, it is recommended in the reinforced concrete beams with FRP that this ratio should be higher than 2 (Figure 4).

Analysis of the load-strain A diagram

In fact, strain A is the strain of the compressive region which is measured in mid-span and at 2 cm from the farthest compressive concrete axis. The diagram of load-negative bending strain is shown in Figure 5. With the analysis of the diagrams, it can be observed that during equal loading, the strain in the compressive zone in RC beams with FRP in comparison with RC beams was applied further and the concrete under less loading was achieved by the rupture. As such, this reason comes up from the low modulus of elasticity of FRP. Also, it can be said that using high strength concrete instead of normal concrete in similar loading, caused a decrease of the created strains and thus, the concrete showed a better

strength on ruptures. Constant ratio of bars and dimension reduction significantly increases the strain of compressive concrete. Also, increase of depth effectively over breadth in these beams with similar ratio of bars, reduced the strain of compressive concrete.

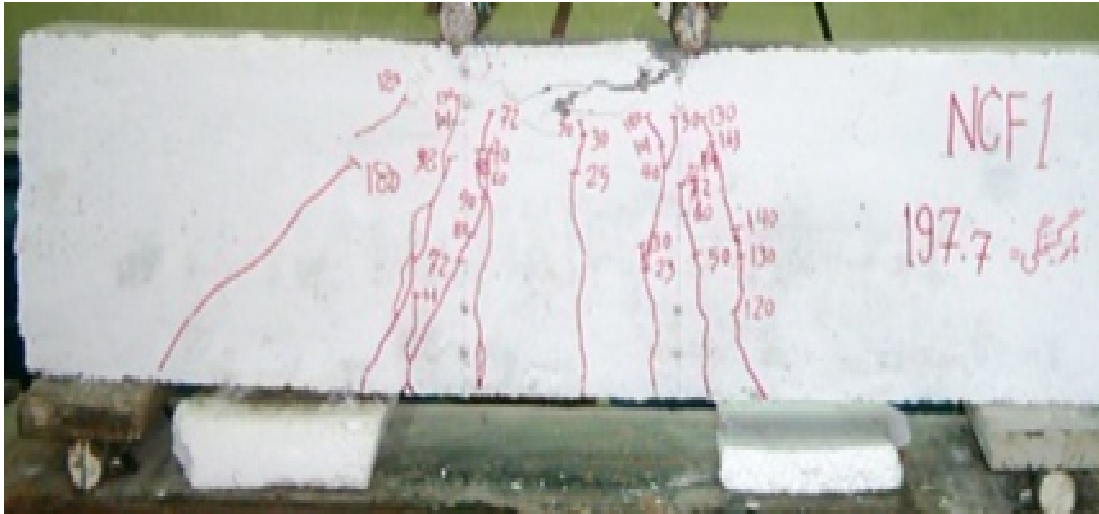
Analysis of the load-strain B diagram

In Figure 6, the compressive and tensile strains have been considered to be positive and negative, respectively. These records show the amount of strain under different loading at 4 cm from the farthest compressive concrete axis. Also, with the assistance of it, it is possible to observe changes of the neutral axis. It can be seen that this axis in RC beams with steel during loading is located above the neutral axis. In addition, using FRP as reinforcements causes the neutral axis to go up due to low modules of elasticity of FRP.

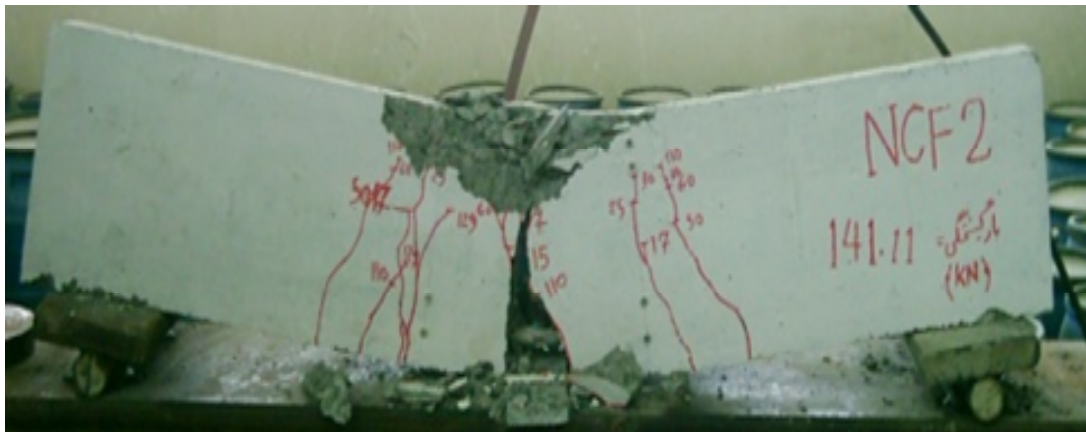
In most of the beams, which used FRP as reinforcement bars, their ruptures occurred at the compressive zone of the concrete, especially on those beams that are made of the normal concrete. It can be seen that the neutral axis goes up and this process continues until ultimate loading; then in the ultimate loading, the neutral axis comes down and continues until failure. Of course, this process in concrete beams made of high strength concrete has been recorded with less intensity. Perhaps, the reason for the downward motion of the neutral axis is that in ultimate loading, the concrete arrives in a non-linear mode and with little stress, more strain will be created; but in FRP bars, the relation of stress-strain is linear. Therefore, for the bending layers to remain flat, it is necessary for the neutral axis to move down. Also, considering more ductility of the normal concrete, a downward movement of the neutral axis is more visible. With the use of diagrams, it can be seen that in beams made of high strength concrete, the position of the neutral axis is located higher than those samples manufactured of normal concrete, which seems neutral considering the strength of the concrete.

Analysis of the load-strain D diagram

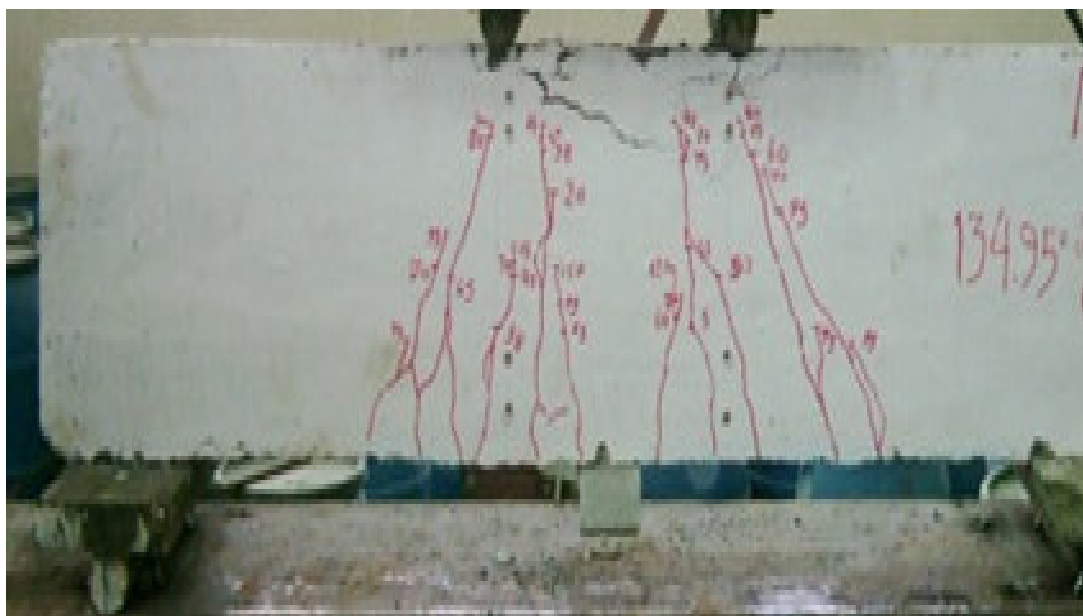
The results of the load-strain C diagram are similar to that of the load-strain D diagram and it shows good adhesion between FRP and the concrete suitable to transfer strains and stresses. So, the analysis of the load-strain D diagram is given in Figure 7. According to Figure 7, in the concrete beams with FRP as reinforcement, the strain on FRP is more than the reinforcement samples with steel. This is due to the low modules of elasticity of FRP. As it is known, low modules of elasticity causes cracks on beams with long width. Also, the load-strain diagram of FRPs is mostly linear and as such, yield point was not seen on them.



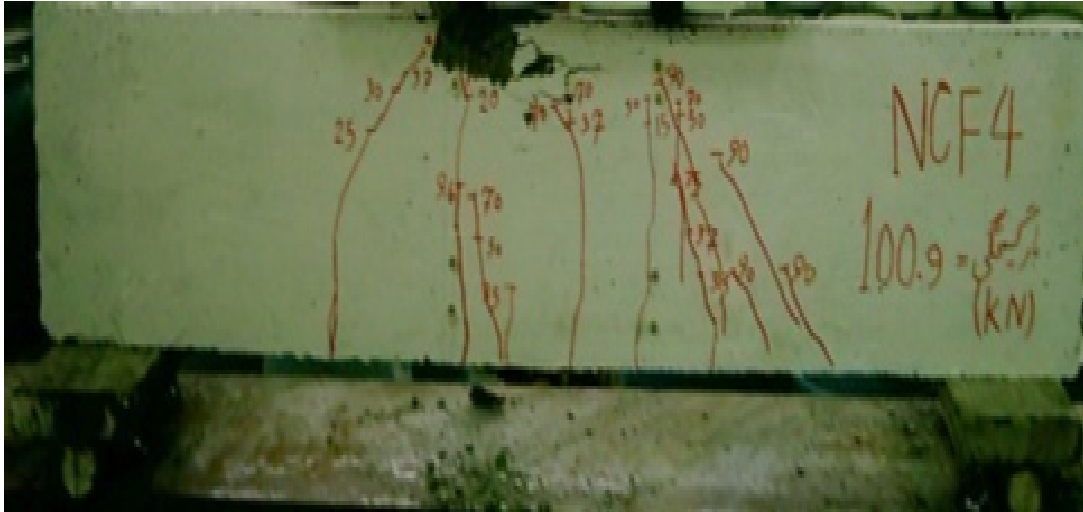
NCF 1.



NCF2



NCF3



NCF4



HCF5



HCF6



HCF7



HCF8

Figure 3. Beams' ruptures.

In the reinforced concrete beams with FRP, the ratio of the bar is $\rho_f = 0.00487$. Thus, the high strength concrete used to replace it in the normal concrete has caused a little decrease on the strain of FRPs. Also, using the compressive steel bar has more reduction effect in the

strain of FRP; but in the FRP reinforced concrete beams, with the ratio of the bar realized as $\rho_f = 0.00745$ and the ratio of the effective depth over breadth realized as $1/7$, the beam behavior which was completely used in the high strength concrete caused a significant increase in

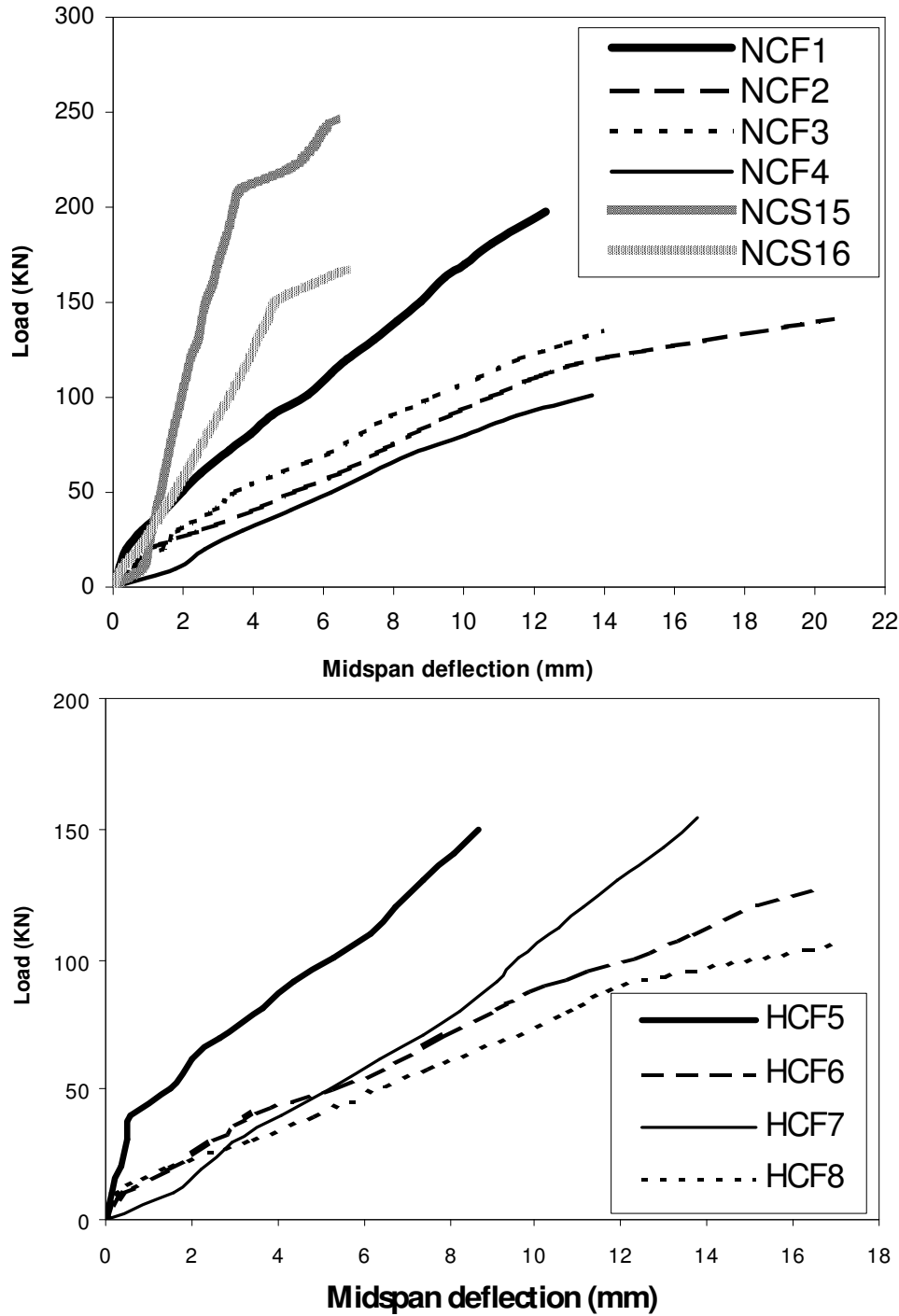


Figure 4. The load-deflection diagram of beams at mid-span.

the strain of FRP. In addition, the compressive steel bar has more additive effect on the strain, while in other specimens with similar ratio of bar and ratio of effective depth over breadth $2/11$, the use of high strength concrete does not have a noticeable effect on the strain of FRP. However, the two diagrams are very close, but the use of steel bar in a beam made of normal concrete

and a beam made of high strength concrete, decreased the strain of FRP in the same amount.

In specimens with ratio of bars $\rho_f = 0.00990$, use of high strength concrete instead of normal concrete caused a significant reduction on FRP strain. Thus, in a case where the beam has more ratio of bar than the balanced

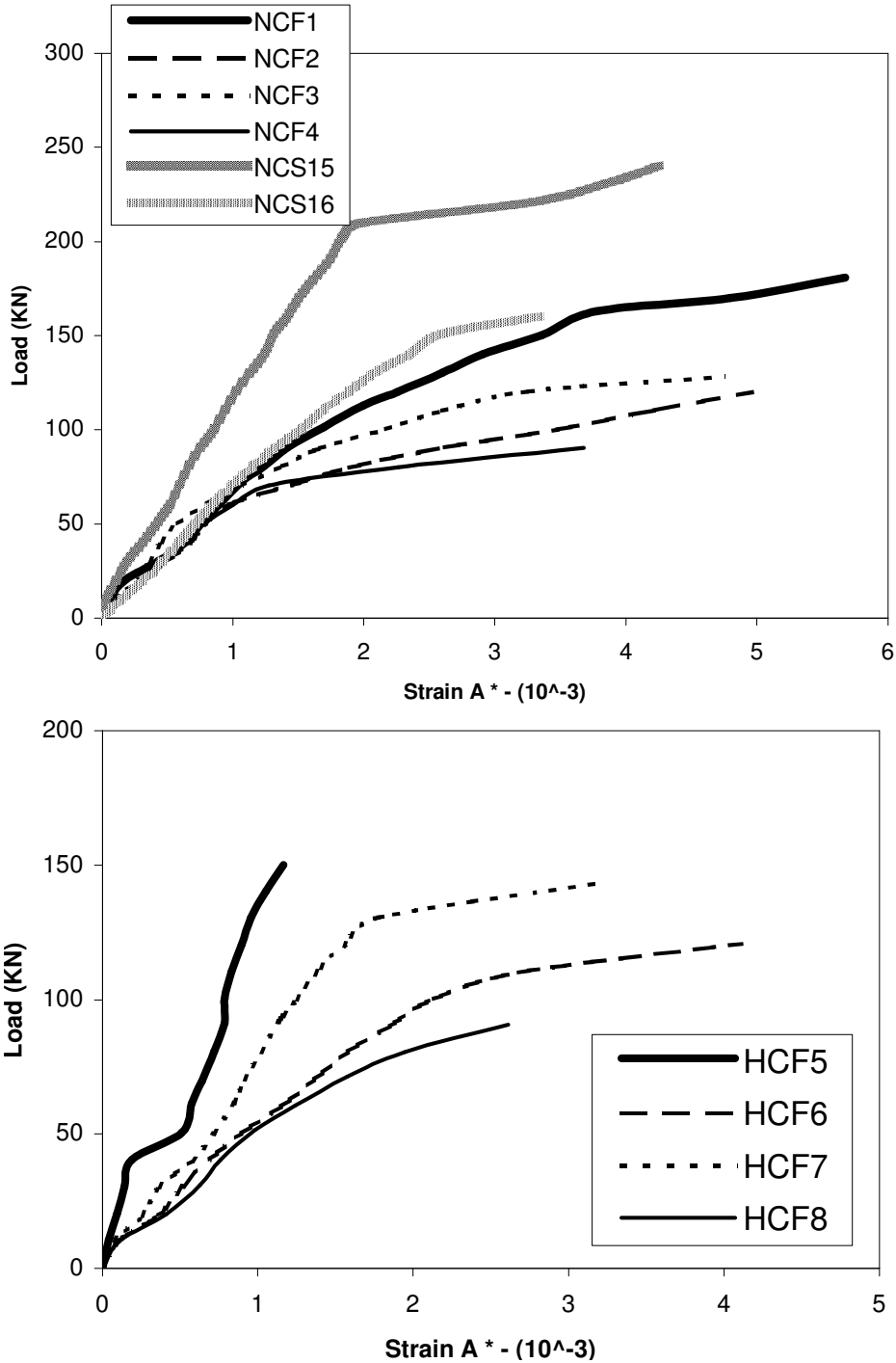


Figure 5. Diagram of the load-negative bending strain A.

mode, the usage of high strength concrete or compressive steel bar are very useful in reducing the created strains.

In beams made from normal concrete with the same diameter of FRP bar, reduction of the section's dimension causes a noticeable increase of FRP strain, but in beams made from high strength concrete and beams made with

compressive steel bar, this status has been seen with less effect. As such, under some loading, the increase in dimension causes a very small reduction in FRP strain. In beams made from normal concrete, increase of effective depth over breadth causes the rise of FRP strain, while in other beams made from high strength concrete and beams made with compressive steel bar, this status does

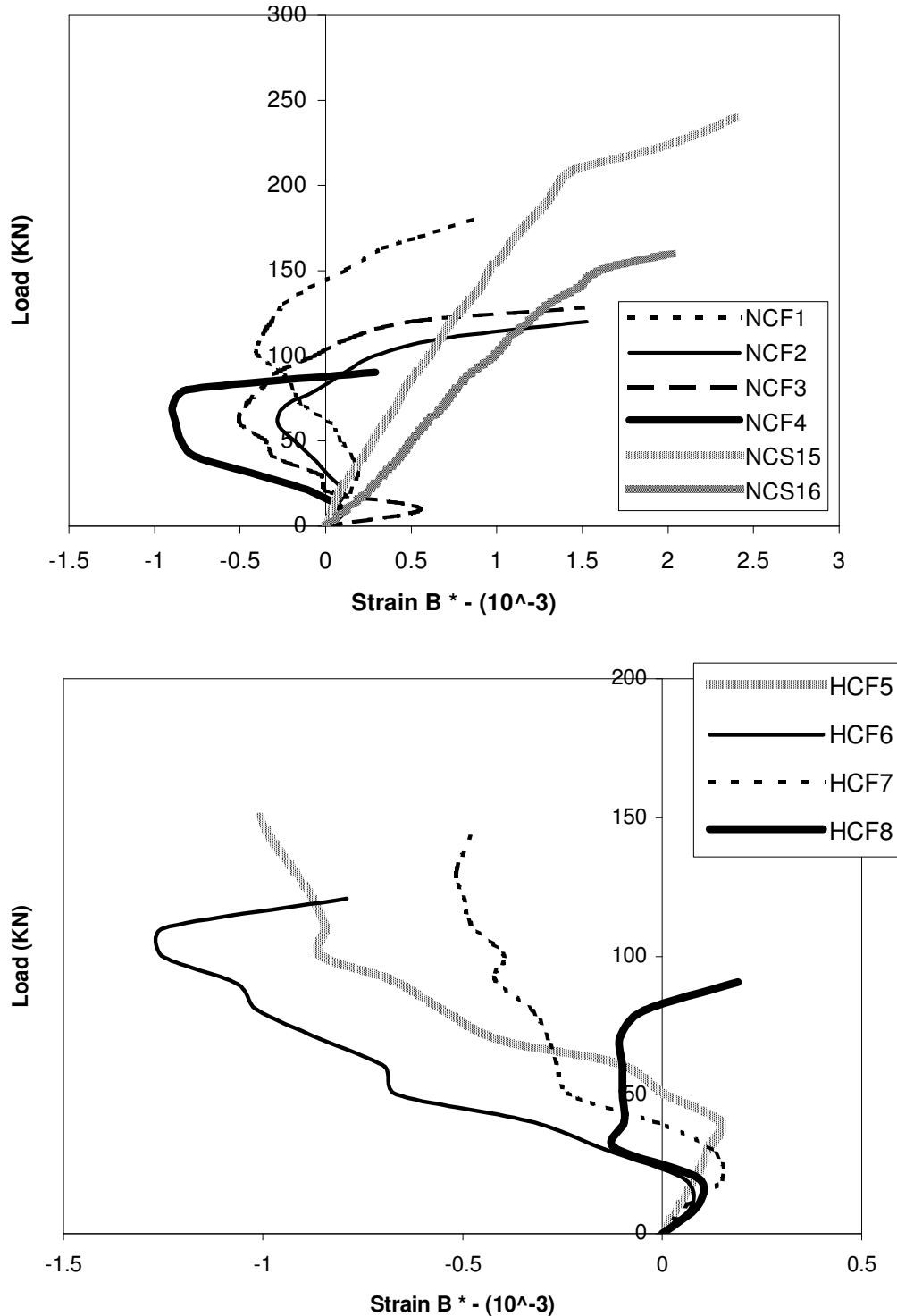


Figure 6. Diagram of the load-negative bending strain B.

not have an important effect on it.

Considering the aforementioned subjects, it can be said that the strain and stress in FRP bar are influenced over different cases such as strength of concrete, ratio of effective depth over breadth, ratio of bars, usage of

compressive steel bar, amount of loading, etc. Therefore, prediction of the exact FRP behavior and kinds of rupture in beams are so difficult, hence the relations provided for designing the reinforced concrete beams with FRP are very conservative (Figure 7).

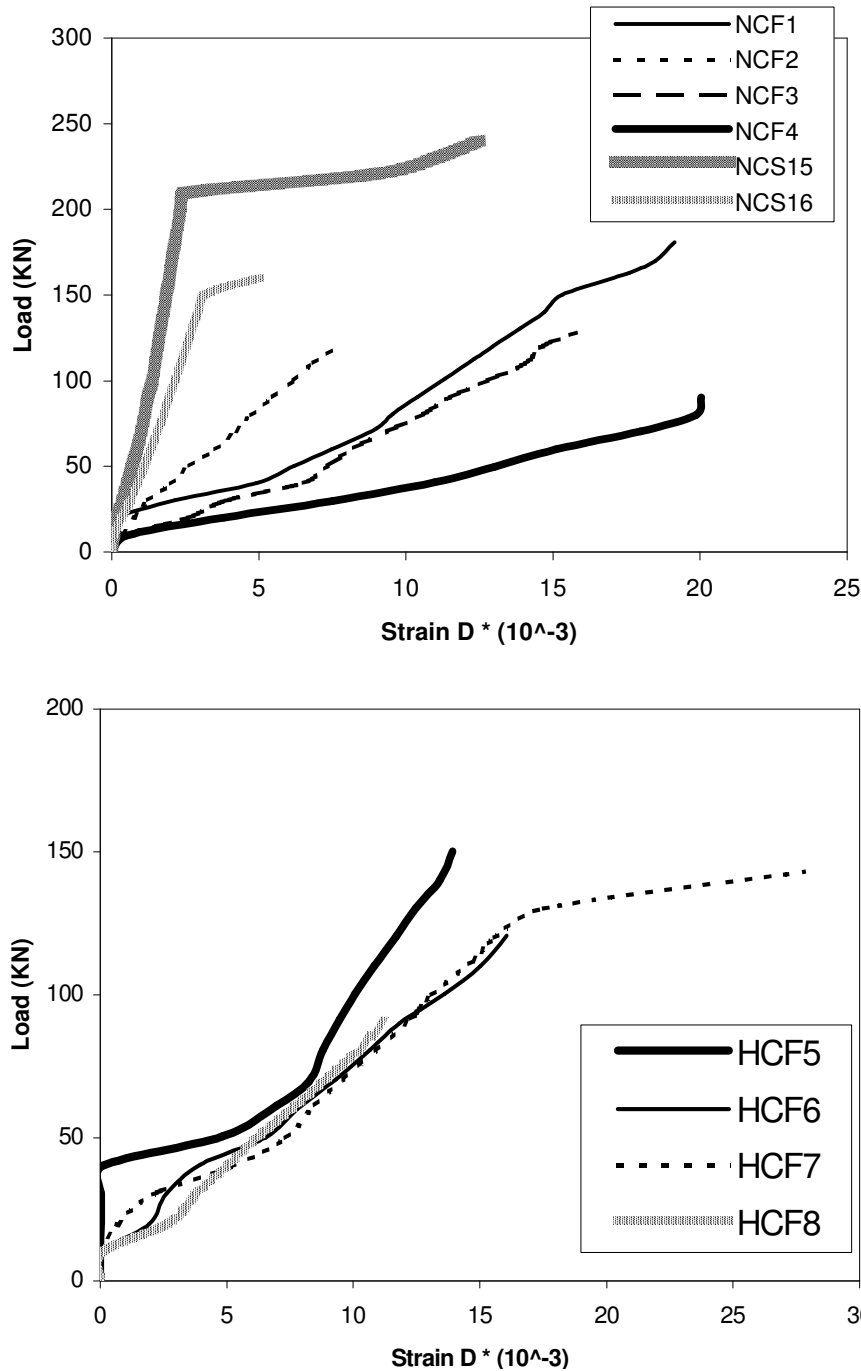


Figure 7. Diagram of the load-bending strain D.

Flexural capacity of beams in comparison with ACI 440

Regarding the computed flexural capacity from ACI 440 equations, it can be said that for constant bar ratios, the reduction of beam sections caused the flexural capacity of the section to decrease. In beams made of normal concrete, in which the bar ratios are less than the

balanced mode, the usage of high strength concrete instead of normal concrete cause a little increase on flexural capacities. Also, in some cases where the beam made of normal concrete with the bar ratio is more than the balanced mode, the usage of high strength concrete cause the computed ratios of the bar for the new section to be less than the ratios in the balanced mode. This case changes the relation in calculating the flexural

Table 5. Summary of the results.

Beams	Ultimate moment capacity by ACI 440	Ultimate loading	Ultimate moment capacity experimental work	Deflection	Load of the first crack	$\frac{M_{ue}}{M_n}$	Kind of ruptures
	$M_n (kN.m)$	$P_{ue} (kN)$	$M_{ue} (kN.m)$	(mm)	(kN)	M_n	
NCF1	10.41	197.71	33.6	12.328	23.466	3.227	Compressive
NCF2	8.854	141.11	23.989	20.518	15.349	2.709	Compressive
NCF3	9.896	134.95	22.942	13.952	12.5	2.318	Compressive
NCF4	9.718	100.94	17.160	13.651	9.642	1.766	Compressive
HCF5	10.527	150.10	25.517	8.691	42	2.424	Rupture in FRP
HCF6	8.948	127.48	21.672	16.723	16.667	2.422	Compressive
HCF7	10	154.05	26.189	13.753	18.203	2.619	*
HCF8	8.422	106.42	18.091	16.964	13.810	2.148	Compressive
NCF15	14.845	246.9	41.973	6.357	40	2.827	Rupture in steel
NCF16	12.095	167.22	28.427	6.656	25	2.350	Rupture in steel

*rupture in concrete and FRP at the same time; beam was broken in two parts.

capacity that is presented by ACI 440, because we have less flexural capacity and used the normal concrete. The submitted relations and equations by ACI 440 are used to compute the flexural capacity in bar ratios less than the balanced mode which are very conservative.

According to the experimental results, it can be observed that in beams with bar ratios less than the balanced mode and in the ratio of effective depth over breadth less than 2, the usage of high strength concrete caused a reduction in the ultimate moment capacity, but in those beams with the ratio of the effective depth over breadth more than 2 (beams in both modes are bigger and less than the bar ratios in the balanced mode), the usage of high strength concrete increases the ultimate moment capacity. Therefore, it is recommended that in concrete beams made of high strength concrete and FRP as reinforcements, the ratio of effective depth over breadth which is more than 2 is selected. In the experimental test that is similar to the theory relations, a reduction of beam sections in beams with constant bar ratios caused a decrease in the ultimate moment capacity. In those beams where FRP was used as reinforcement, ultimate moment capacities were significantly less than those specimens made of steel.

Considering the results that come from the experimental works, the presented ρ_f by ACI 440 cannot be the exact criteria for detecting the kind of failure, because in a lot of cases where bar ratios were less than the balanced mode, rupture occurred from the compressive area of the concrete. Therefore, regarding the results of experiments, it can be recommended that $0.56\rho_b$ is to determine the exact criteria of failure. By comparing the ratio of the ultimate moment capacity that comes from the experiments and the nominal moment capacity submitted by ACI 440, it is seen that the said ratio reduced due to a decrease in the bar ratios.

This means that with a decrease in the bar ratios, ACI 440 acts more conservative. Regarding ACI 440, this ratio for the mode that is less than the balanced mode is considerably larger than the mode that is more than the balanced mode.

Also, an increase in the strength of concrete in most of the cases caused a reduction of this ratio. As it can be seen in Table 5, this ratio for FRP bars is bigger than the steel reference samples. Meanwhile, ACI 440 has been considered a reduction coefficient for nominal moment capacity of sections. As an example, the bar ratio that is less than the balanced mode is 0.5. Including these coefficients in the experiments, it can be said that ACI has been considered as the allowed flexural capacity for the bar ratio that is less than the balanced mode, which is around one fifth of the actual flexural capacity and has been shown in Table 5.

Conclusion

1. Deflection of beams, width of cracks and their extent in the reinforced concrete beams with FRP in comparison with the reference reinforced samples amid steel.
2. The load-deflection diagram of the reinforced beams with FRP is like a straight line and there is no failure found on it. As such, an increase in concrete strength does not have any effect on deflections. When the diameter of the bar is constant, a reduction of beams' dimension caused a significant increase in the deflection of beams.
3. In FRP reinforced concrete beams where a diameter of the bars is constant, the load of the first crack will be reduced due to a decrease in the dimensions of beams.
4. Usage of high strength concrete instead of normal concrete creates more cracks, but less width in the reinforced concrete beams with FRP.

5. In some FRP reinforced concrete beams, especially in those beams made of normal concrete, it is observed that the neutral axis moves up due to the creation of cracks and this process continues until ultimate loading. Then, in ultimate loading, the neutral axis comes down until a final rupture of the beam.

6. The reinforced concrete beams with FRP have an elastic behavior of beams, and after load removal, a major deflection can be seen to go backwards.

7. It is recommended that the ratio of effective depth over breadth that is more than 2 is selected in the reinforced concrete beams, especially in those beams manufactured by high strength concrete.

8. The presented bar ratio ρ_b by ACI 440 is not the exact criterion to recognize the type of failure. Therefore, according to the tests results, $0.56\rho_b$ is a more accurate criterion to determine the type of failure that is proposed.

REFERENCES

- ACI Committee 318 (1999). Building Code Requirements for Struct Concrete (ACI 318-99) and Commentary(318R-99). Am. Concrete Institute, Farmington Hills, Mich., p. 391.
- ACI Committee 440 (2001). Guide for the Design and Construction of Concrete Reinforced with FRP Bars (ACI 440.1R-01). Am. Concrete Institute, Farmington Hills, Mich., p. 41.
- AIMusallam TH, Al-Salloum YA, Alsayed SH, Amjad MA (1997). Behavior of concrete beams doubly reinforced by FRP bars. In: Proceedings of the third Int. symposium on non-metallic (FRP) reinforcement for concrete structures (FRPRCS-3), Japan. 2: 471–78.
- Alsayed SH (1998). Flexural behaviour of concrete beams reinforced with GFRP bars. *Cem. Concr. Compos.*, 20: 1–11.
- Alsayed SH, Al-Salloum YA, AIMusallam TH (1997). Shear design for beams reinforced by GFRP bars. In: Proceedings of the third int. symposium on non-metallic (FRP) reinforcement for concrete structures (FRPRCS-3), Japan., 2: 285–92.
- Benmokrane B, Chaallal O, Masmoudi R (1995). Glass fibre reinforced plastic (GFRP) rebars for concrete structures. *Constr. Build. Mater.*, 9: 353–364.
- Benmokrane B, Chaallal O, Masmoudi R (1996). Flexural response of concrete beams reinforced with FRP reinforcing bars. *ACI Struct. J.*, 91: 46–55.
- Brown VL, Bartholomew CL (1993). FRP reinforcing bars in reinforced concrete members. *ACI Mater. J.*, 90: 34–39.
- Deitz DH, Harik IE, Gesund H (1999). One-way slabs reinforced with glass fiber reinforced polymer reinforcing bars. In: *ACI proceedings, the fourth int. symposium, Detroit*, pp. 279–286.
- Duranovic N, Pilakoutas K, Waldron P (1997). Tests on concrete beams reinforced with galss fibre reinforced plastic bars. In: *Proceedings of the third int. symposium on non-metallic (FRP) reinforcement for concrete structures (FRPRCS-3) Japan*. 2: 479–486.
- Faza SS, GangaRao HVS (1993). *Glass FRP Reinforcing Bars for Concrete*. Elsevier Science Publishers B. V. All right reserved, pp. 167-188.
- Grace NF, Soliman AK, Abdel-Sayed G, Saleh KR (1998). Behavior and ductility of simple and continuous FRP reinforced beams. *J. Compos. Constr.*, 2: 186–194.
- Masmoudi R, Thériault M, Benmokrane B (1998). Flexural behavior of concrete beams reinforced with deformed fiber reinforced plastic reinforcing rods. *ACI Struct. J.*, 95: 665–676.
- Michaluk CR, Rizkalla SH, Tadros G, Benmokrane B (1998). Flexural behavior of one-way concrete slabs reinforced by fiber reinforced plastic reinforcements, *ACI Struct. J.*, 95: 353–365.
- Pecce M, Manfredi G, Cosenza E (2000). Experimental response and code models of GFRP RC beams in bending. *J.Compos. Constr.*, 4: 182-190.
- Saadatmanesh H, Ehsani MR (1991). Fiber Composite Bar for Reinforced Concrete Construction. *J. Compos. Mater.*, 25: 188-203.
- Thériault M, Benmokrane B (1998). Effects of FRP reinforcement ratio and concrete strength on flexural behavior of concrete beams. *J. Compos. Constr.*, 2: 7–16.
- Tureyen AK, Frosch RJ (2002). Shear tests of FRP-reinforced concrete beams without stirrups. *ACI Struct. J.*, 99: 427–434.
- Victor C, Shuxin W (2002). Flexural Behavior of Glass Fiber-Reinforced Polymer (GFRP) Reinforced Engineered Cementitious Beams. *ACI Struct. J.*, pp. 11-21.
- Vijay PV, GangaRao HVS (2001). Bending Behavior and Deformability of Glass Fiber-Reinforced Polymer Reinforced Concrete Members. *ACI Struct. J.*, pp. 834-842.
- Yost JR, Goodspeed CH, Schmeckpeper ER (2001). Flexural performance of concrete beams reinforced with FRP grids. *J. Compos. Constr.*, 5: 18–25.
- Yost JR, Gross SP, Dinehart DW (2001). Shear strength of normal strength concrete beams reinforced with deformed GFRP bars. *J. Compos. Constr.*, 5: 268–275.
- Yost JR, Gross SP (2002). Flexural Design Methodology for Concrete Beams Reinforced with Fiber-Reinforced Polymers. *ACI Struct. J.*, pp. 308-316.